Theor Chem Acc (2011) 129:615–623
DOI 10.1007/s00214-011-0909-9

REGULAR ARTICLE

Divalent Pb(0) compounds

Nozomi Takagi · Gernot Frenking

Received: 5 November 2010 / Accepted: 10 February 2011 / Published online: 26 February 2011

Abstract Density functional theory (DFT) calculations have been carried out on four novel dicoordinated lead compounds PbL_2 where L is an N-heterocyclic ylidene or a five-membered cyclic ylidene (**1Pb**, **2Pb**, **4Pb**, **5Pb**) and for a plumbylene-coordinated carbone CL_2 (**3Pb**). The theoretically predicted equilibrium geometries and the first and second proton affinities of **1Pb**–**5Pb** are reported. Geometry optimizations have also been carried out for the complexes with one and two BH_3 ligands **1Pb(BH$_3$)**–**5Pb(BH$_3$)** and **1Pb(BH$_3$)$_2$**–**5Pb(BH$_3$)$_2$**, and for the transition metal complexes **1PbW(CO)$_5$**–**5PbW(CO)$_5$** and **1PbNi(CO)$_3$**–**5PbNi(CO)$_3$**. The results suggest that the molecules **1Pb**, **2Pb** and **4Pb** possess properties which identify them as divalent Pb(0) compounds (plumbylones). This comes to the fore by the theoretically predicted second PAs which are very large for a lead compound and (for **1Pb** and **4Pb**) by the BDE of the second BH_3 ligand. Compound **3Pb** should be considered as a plumbylene-coordinated divalent C(0) compound (carbone) which has a very high second PA of 195.1 kcal/mol. The geometry optimization of **5Pb** gives an equilibrium structure which identifies the molecules as divalent Pb(II) compound, i.e., as a plumbylene.

Keywords Divalent Pb(0) compounds · Plumbylone · Proton affinity · Transition metal complexes · DFT calculations

Dedicated to Professor Pekka Pyykkö on the occasion of his 70th birthday and published as part of the Pyykkö Festschrift Issue.

N. Takagi · G. Frenking (✉)
Fachbereich Chemie, Philipps-Universität,
Hans-Meerwein-Straße, 35032 Marburg, Germany
e-mail: frenking@chemie.uni-marburg.de

1 Introduction

The chemistry of divalent carbon(0) compounds CL_2 where L is a strong σ-donor ligand has been widely expanded, and it has attracted much interest in recent years [1–12] after the peculiar donor–acceptor bonding situation L → C ← L had been recognized [13–18]. The term carbones has been suggested for compounds CL_2 [17] which unlike carbenes CR_2 have two lone-pair orbitals at carbon and thus are σ-donors and π-donors while carbenes are σ-donors and π-acceptors. While carbodiphosphoranes $C(PR_3)_2$ [19] are known since 1961 [20], new carbones such as carbodicarbenes $C(NHC)_2$ (NHC = N-heterocyclic carbene) [21–23] and carbodiylides $C(ECp^*)_2$ (E = B–Tl) [24, 25] were theoretically predicted. Carbodicarbenes could in the meantime become synthesized [1, 2], and they are currently a topic of intensive investigations [1–12].

Theoretical investigations into the heavier group-14 homologues EL_2 (E = Si, Ge, Sn) showed that the donor–acceptor bonding model is also valid for tetrole compounds L → E ← L [26, 27]. It was suggested that the previously synthesized trisilallene and trigermaallene [28–30] (Scheme 1) which have strongly bent E–E′–E moieties with bonding angles of ~130° should rather be considered as divalent E(0) compounds [26, 27]. The bonding situation in the molecules is better described in terms of donor–acceptor interactions E → E′ ← E (Scheme 1b) rather than E=E′=E (Scheme 1a). Theoretical studies showed that the parent "allenes" H_2EEEH_2 are even more strongly bent with bonding angles E–E–E of ~75° [31–34]. It thus seems that the donor–acceptor model L → E ← L is even more valid for the heavier tetrole elements Si–Sn than for carbon. This finding could be explained with the singlet–triplet gaps of atom E and fragment ER_2 in R_2EEER_2

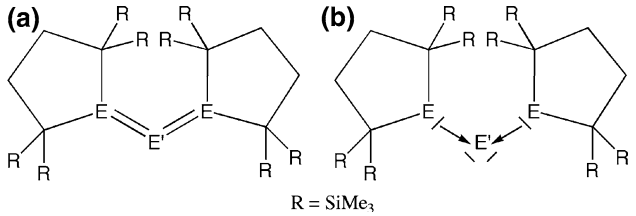

Scheme 1 Schematic view of the trisilaallene (E=E′=Si), trigermaallene (E=E′=Ge) and 1,3-digermasilaallene (E=Ge; E′=Si). **a** Bonding situation suggested in references [28–30]. **b** Bonding situation suggested in references [26, 27]

which favour the singlet states and thus the donor–acceptor bonding for the heavier group-14 atoms [26].

In this work, we report calculated results of divalent E(0) compounds for the heaviest tetrole atom lead PbL_2 which have not been reported before. The study is an extension of our previous investigations [26, 27] of EL_2 (E = Si–Sn) where we employed the same kind of ligands L as in this work. Scheme 2 schematically shows the calculated compounds **1Pb–5Pb** which are not known yet experimentally. We address the question whether the compounds **1Pb–5Pb** should be interpreted as divalent Pb(0) compounds (plumbylones). The divalent Pb(0) character is evaluated by the optimized geometries, the shape of the frontier orbitals, and the calculated first and second proton affinities. The ability to serve as double donors which comes from the two lone-pairs at lead has been further investigated. We calculated the complexes of **1Pb–5Pb** as electron donors and the Lewis acid BH_3. We also calculated complexes of **1Pb–5Pb** with $W(CO)_5$, and $Ni(CO)_3$ which may serve as a guideline for synthesizing the molecules.

2 Computational details

All geometries were optimized at the gradient-corrected density functional theory (DFT) level of theory using Becke's exchange functional [35] in conjugation with Perdew's correlation functional [36] with split-valence basis sets of doubly polarized triple-ζ-quality developed by Weigend and Ahlriches which are donated as BP86/TZVPP using the program TurboMole6.1 [37, 38]. Relativistic effects were considered by introducing effective core potentials for the heavy elements Pb, Ni and W [39]. Stationary points were characterized as minima on the potential energy surface by calculating the Hessian matrix analytically at this level. Thermodynamic corrections have been taken from these calculations. The standard state for the proton affinities and bond dissociation energies is 298.15 K and 1 atm. The full sets of calculated geometries and energies are given in Supporting Information.

3 Parent compounds 1Pb–5Pb

The optimized geometries with the important geometrical parameters of the parent compounds **1Pb–5Pb** are shown in Fig. 1.

Compound **1Pb** is composed of a Pb atom and two N-heterocyclic plumbylene ligands (NHPb). Figure 1 shows that **1Pb** has a rather unusual equilibrium geometry which differs significantly from the geometries of the lighter homologues **1E** (E = Si–Sn) [26, 27]. The Pb–Pb–Pb angle in **1Pb** is rather wide (128.5°) while the E–E–E angles in **1E** are much more acute (73.6° in **1Si**, 81.2° in **1Ge**, 85.4° in **1Sn**). On the other hand, the NHPb ligands in **1Pb** are strongly tilted towards dicoordinated lead atom (Fig. 1) with a side-on coordination of the ligands, while the NHE (E = C–Sn) ligands in the lighter homologues are coordinated in a head-on fashion. The geometry of **1Pb** suggests that the bonding of the NHPb ligands to the central lead atom takes place through the p(π) orbital of the ligand, while the bonding in the lighter homologues comes from the σ-donor orbital of the ligand atom E [26, 27].

The latter conclusion is supported by the calculate energy levels of the highest lying σ- and π-donor orbitals of NHE. Table 1 shows that the σ-lone-pair MO is the highest lying orbital (HOMO) in NHC while the HOMO in the heavier homologues NHE (E = Si–Pb) are π-orbitals. The energy level of the latter MO continuously increases from carbon to lead while the σ-lone-pair MO becomes lower in energy. The latter orbital remains the dominant donor orbital for the NHE → E ← NHE bonding when E = Si–Sn because of the better overlap but the situation changes in

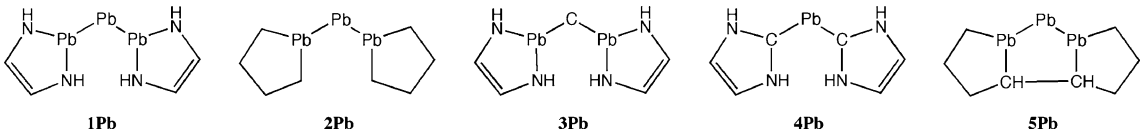

Scheme 2 Overview of the calculated compounds **1Pb–5Pb**. The figure of **5Pb** shows the starting structure of the geometry optimization which yields a compound where the Pb–CH bonds are broken. The optimized molecule is a monocyclic species with three dicoordinated lead atoms (Fig. 1)

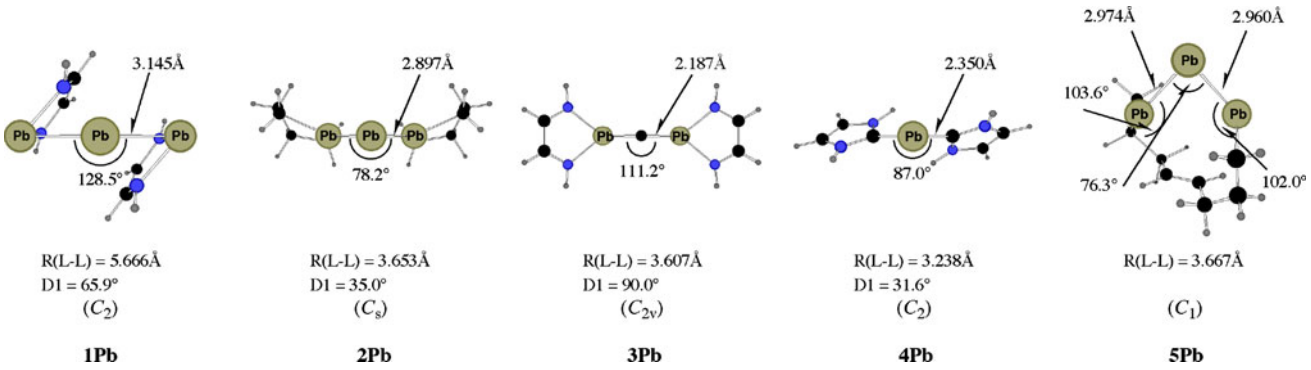

Fig. 1 Optimized geometries of the parent compounds **1Pb–5Pb** at BP86/TZVPP showing the most important geometrical parameters. Distances are given in Å, angles in degree. The value for R(L–L) gives the interatomic distance between the terminal lead atoms. The torsion angle D1 given in each structure is defined as the interplanar angle between the central E–E–E plane and the plane of the bonded ligand:

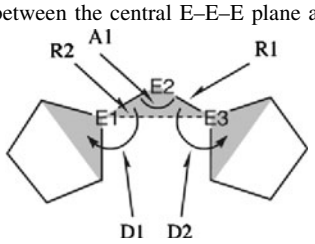

Table 1 Frontier orbital energies (in eV) and energy differences between the lowest lying singlet and triplet states of the ligands at BP86/TZVPP including ZPE corrections (in kcal/mol)

E=	C	Si	Ge	Sn	Pb
			N-heterocyclic ylidene		
			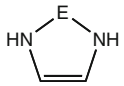		
Singlet	0.0 (C_{2v})	0.0 (C_{2v})	0.0 (C_{2v})	0.0 (C_{2v})	0.0 (C_{2v})
HOMO	−4.95 (σ)	−4.83 (π)	−4.54 (π)	−4.20 (π)	−3.94 (π)
HOMO-1	−5.82 (π)	−5.86 (σ)	−6.30 (σ)	−6.41 (σ)	−6.76 (σ)[a]
Triplet	+80.6 (C_s)	+58.7 (C_s)	+48.4 (C_s)	+35.5 (C_s)	+29.1 (C_s)
			1-cyclopentylidene		
					
Singlet	0.0 (C_2)	0.0 (C_2)	0.0 (C_2)	0.0 (C_2)	0.0 (C_2)
HOMO	−4.67 (σ)	−5.10 (σ)	−5.17 (σ)	−5.06 (σ)	−5.00 (σ)
Triplet	+7.1 (C_2)	+27.0 (C_2)	+30.8 (C_2)	+30.7 (C_2)	+33.0 (C_2)

[a] HOMO-2

1Pb where the NHPb → Pb ← NHPb interactions mainly take places through the π-donor orbitals of NHPb.

Unlike **1Pb**, the geometry of **2Pb** resembles the equilibrium structures of the lighter homologues **2E** [26, 27]. Figure 1 shows that the bonding angle Pb–Pb–Pb angle in **2Pb** (78.2°) is very similar to the values which are calculated for **2E** (76.5° in **2Si**, 79.4° in **2Ge**, 76.4° in **2Sn**). The shape of **2Pb** suggests that the bonding of the plumbylene ligands to the central divalent Pb(0) atom takes places via the σ-lone-pair donor orbital of the divalent Pb(II) atoms of the ligands. Table 1 shows that the energy level of the σ-lone-pair donor orbital of the 1-cyclopentylidene ligand increases slightly from Si (−5.10 eV) to Pb (−5.00 eV).

The equilibrium geometries of the lead compounds **3Pb** and **4Pb** are also very similar to the calculated structures of the lighter homologues **3E** and **4E** [26, 27] and thus shall not be discussed in detail. The optimized structure of **5Pb**, however, is quite different from the equilibrium geometries of **5C–5Sn**. The Pb–CH bonds (Scheme 1) break during the geometry optimization which yields a monocyclic ring with a C=C double bond and three divalent lead atoms (Fig. 1). The optimized structure which is shown in Fig. 1 exhibits a *trans* conformation of the C=C double bond. We also optimized a *cis* form of **5Pb** which is predicted to be 6.9 kcal/mol higher in energy than the *trans* form.

The molecular orbitals of **1Pb–5Pb** shall be visually inspected to see whether the typical features of divalent Pb(0) compounds (plumbylones) can become identified through the occurrence of two lone-pair orbitals with σ- and π-symmetries[1] at the central Pb atom. In case of **3Pb** the central divalent atom is carbon which means that the molecule may be a carbodiplumbylene. Figure 2 shows the plots of the relevant highest lying MOs. The π-type (see footnote 1) HOMO of all molecules **1Pb–5Pb** has the largest coefficient at the central dicoordinated atom and may become classified as lone-pair orbital. The

[1] There are no genuine σ or π orbitals in **1Pb–5Pb** because the molecules have no mirror plane. However, the shape of the MOs resembles σ- or π-type orbitals which are symmetric or antisymmetric with respect to a local plane of the central E–E′–E moiety.

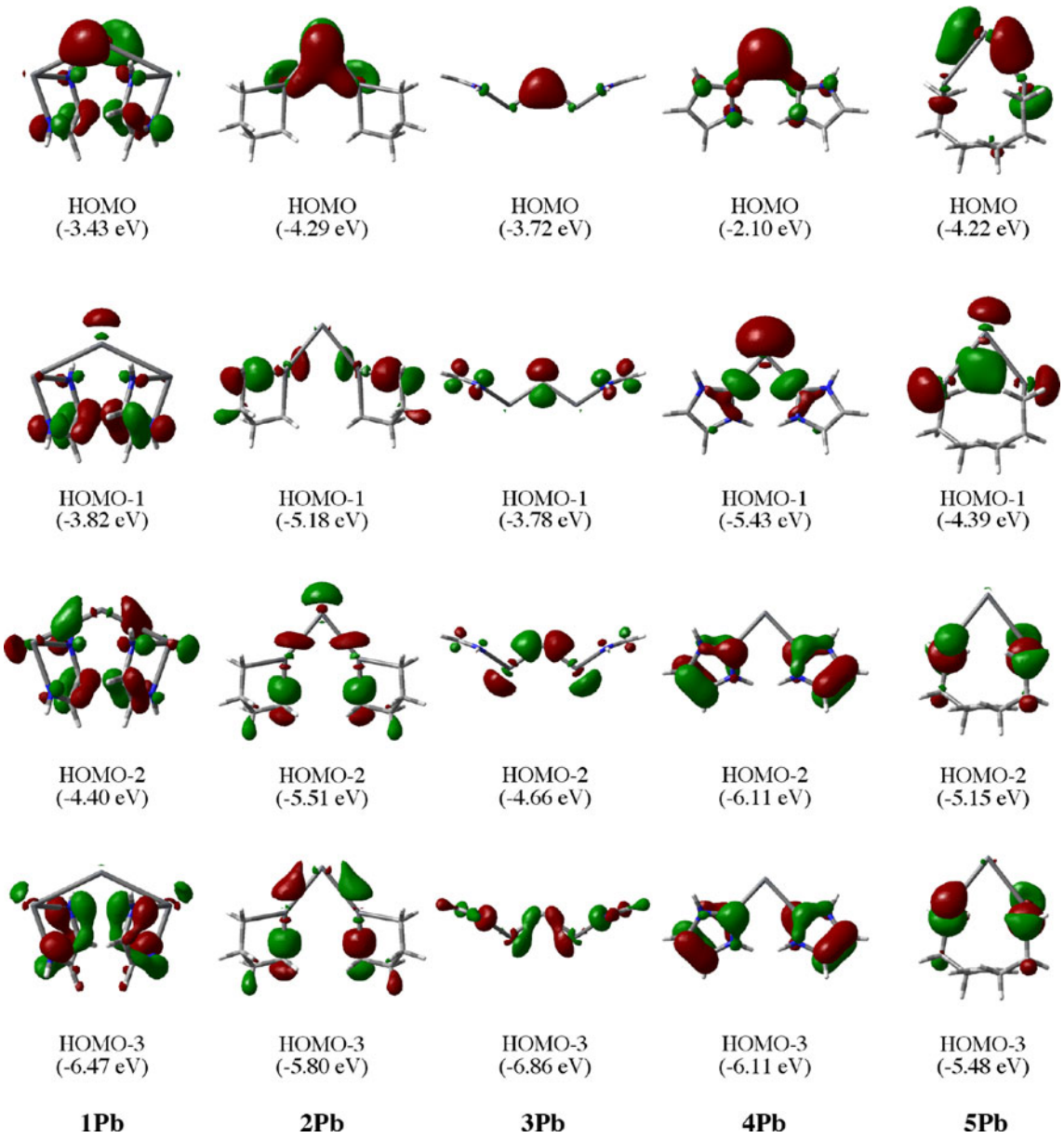

Fig. 2 Plot of the highest lying occupied molecular orbitals of **1Pb–5Pb** that are relevant for the discussion

identification of a σ-type lone-pair MO is more difficult. Except for the HOMO-1 of **4Pb**, there is no orbital which may be considered as σ-type lone-pair MO. The occupied valence orbitals which are shown in Fig. 2 are strongly delocalized. The shape of the highest occupied orbitals does not support the classification of the lead compounds as plumbylones except, perhaps, for **4Pb**.

4 Singly and doubly protonated compounds

A typical feature of divalent E(0) compounds is a high first *and* a high second proton affinity (PA). Our previous calculations of the lighter homologues **1E–5E** (E = C–Sn) showed that all species have large values for the second PA which could be related to the occurrence of two lone-pair MOs at the divalent atom E [26, 27]. Figure 3 shows the optimized geometries of the singly and doubly protonated compounds **1Pb(H$^+$)–5Pb(H$^+$)** and **1Pb(H$^+$)$_2$–5Pb(H$^+$)$_2$**. Table 2 gives the calculated values for the first and second PA of the lead compounds. The data for the lighter homologues where E = C–Sn are given for comparison.

The geometries of the singly protonated species **1Pb(H$^+$)**, **2Pb(H$^+$)** and **4Pb(H$^+$)** show that the proton is bonded to the π-orbital while the proton which is attached to the carbon atom in **3Pb(H$^+$)** is bonded to the σ-orbital.

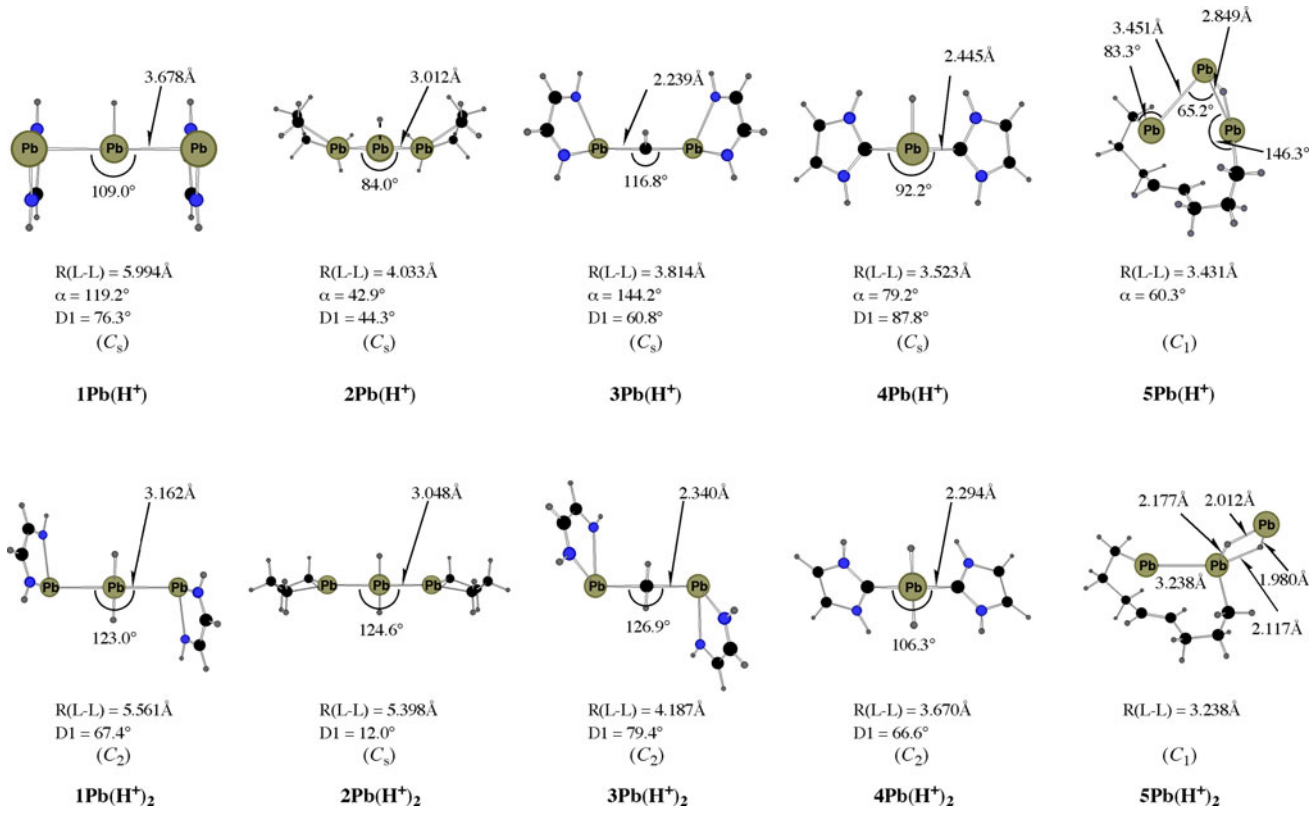

Fig. 3 Optimized geometries of the singly and doubly protonated cations **1Pb(H^+)–5Pb(H^+)** (top) and **1Pb(H^+)$_2$–5Pb(H^+)$_2$** (bottom) at BP86/TZVPP showing the most important geometrical parameters. Distances are given in Å, angles in degree. The value for R(L–L) gives the interatomic distance between the terminal lead atoms. The angle α gives the bending angle of the Pb–H^+ bond with respect to the central E–E–E plane. For the definition of the torsion angle D1 see Fig. 1

The same result was found for the lighter homologues where E = Si–Sn [26, 27]. The proton in **5Pb(H^+)** is in a bridging position between two lead atoms. This may be due to the structure of the parent compound **5Pb** which has a different geometry and bonding situation of the central dicoordinated atom Pb compared with E = Si–Sn. The diprotonated species **1Pb(H^+)$_2$–4Pb(H^+)$_2$** exhibit a similar tetrahedral arrangement at the central group-14 atom as the lighter homologues **1E(H^+)$_2$–4E(H^+)$_2$**. The compound **5Pb(H^+)$_2$** has two doubly bridging protons between the same pair of lead atoms. A geometry optimization of **5Pb(H^+)$_2$** where the protons are bridging adjacent pairs of lead atoms was found to be 8.3 kcal/mol higher in energy.

Table 2 shows that the first PAs of **1Pb–5Pb** have similarly high values as the first PA of the tin compounds **1Sn–5Sn**, which means that the lead compounds are rather basic. The second PAs of **1Pb–5Pb** are slightly lower than for **1Sn–5Sn** except for **3Pb** which has a central carbon atoms and for **5Pb** which has a different structure as **4Sn**. Note that the second PA of **3E** increases for atoms E with Si < Ge < Sn < Pb which can be explained with the lowering of the electronegativity and thus with the stronger E → C ← E donation when E becomes heavier. The second PAs of **1Pb–5Pb** are large enough that it seems possible to isolate the doubly protonated species **1Pb(H^+)$_2$–5Pb(H^+)$_2$** as cations of suitable salt compounds.

5 Complexes with BH_3

The rather high second PAs of **1Pb–5Pb**, let it seem feasible that the divalent lead compounds may also bind not only one but two larger Lewis acids such as BH_3. We therefore calculated the complexes with borane ligands **1Pb(BH_3)–5Pb(BH_3)** and **1Pb(BH_3)$_2$–5Pb(BH_3)$_2$**. The optimized geometries of the complexes are shown in Fig. 4. The theoretically predicted BDEs are given in Table 2.

The calculated equilibrium structures show that the BH_3 ligands which bind to the central lead atom have also rather close contacts with the plumbylene lead atoms. This holds for the complexes with one borane ligand **1Pb(BH_3)**, **2Pb(BH_3)** and **5Pb(BH_3)**. The compound **3Pb(BH_3)** is actually not a borane complex, and the geometry optimization yields a structure where an oxidative addition of BH_3 to the divalent carbon atom takes place which gives a molecule with a central tetravalent carbon atom (Fig. 4).

Table 2 First and second proton affinities (PAs) and bond dissociation energies (BDEs) including ZPE corrections for complexes of **1E–5E** (E = C–Pb) with one and two BH_3 ligands and one metal carbonyls $W(CO)_5$ and $Ni(CO)_3$ at 298 K [kcal/mol]

	1E	2E	3E	4E	5E
E = C[a]					
First PA (298 K)	289.2	236.9	same as 1C	same as 1C	280.2
Second PA (298 K)	148.4	87.6			73.8
D_o^{298} (BH_3)	60.2	6.9			55.3
D_o^{298} (BH_3)$_2$	19.4	Diss.[b]			Diss.[b]
E = Si[a]					
First PA (298 K)	249.7	237.9	261.8	275.9	228.8
Second PA (298 K)	142.9	129.3	145.3	166.7	123.9
D_o^{298} (BH_3)	28.3	31.6	34.6	40.8	23.2
D_o^{298} (BH_3)$_2$	26.2	36.3	47.8	48.1	36.6
D_o^{298} [$W(CO)_5$]	41.2	42.0	38.5	53.0	37.9
D_o^{298} [$Ni(CO)_3$]	27.8	27.5	23.0	36.1	24.6
E = Ge[a]					
First PA (298 K)	255.0	229.9	263.9	275.7	220.3
Second PA (298 K)	141.3	127.6	173.8	154.0	120.9
D_o^{298} (BH_3)	27.0	20.7	39.7	39.4	26.3
D_o^{298} (BH_3)$_2$	27.9	29.4	30.9	43.4	16.5
D_o^{298} [$W(CO)_5$]	45.0	35.9	41.1	54.0	31.0
D_o^{298} [$Ni(CO)_3$]	28.3	20.5	25.2	36.3	17.7
E = Sn[a]					
First PA (298 K)	260.9	226.0	276.8	277.9	225.7
Second PA (298 K)	143.6	129.6	194.8	141.5	112.4
D_o^{298} (BH_3)	29.4	23.3	49.1	40.6	23.8
D_o^{298} (BH_3)$_2$	25.1	15.2	47.4	36.0	10.6
D_o^{298} [$W(CO)_5$]	53.5	30.6	53.9	59.5	28.6
D_o^{298} [$Ni(CO)_3$]	36.7	18.1	34.4	41.1	16.3
E = Pb					
First PA (298 K)	251.0	229.4	282.9	273.8	230.8
Second PA (298 K)	138.1	117.2	195.1	114.9	136.0
D_o^{298} (BH_3)	22.3	21.6	100.4[c]	38.5	11.8
D_o^{298} (BH_3)$_2$	21.4	4.0	9.6	28.2	7.6
D_o^{298} [$W(CO)_5$]	43.7	38.9	68.9	60.4	35.7
D_o^{298} [$Ni(CO)_3$]	27.4	28.4	39.1	41.2	28.8

[a] Taken from Ref. [26, 27]

[b] The BH_3 ligand does not bind to the divalent carbon atom. It dissociates during the optimization

[c] The hydrogen atom on the BH_3 group is transferred to the central carbon atom

The calculated BDEs suggest that the BH_3 ligand is more weakly bonded to the lead compounds compared with the tin homologues (Table 2) except for **3Pb(BH$_3$)** which unlike **3Sn(BH$_3$)** is not a borane complex, however. The theoretically predicted BDEs of the BH_3 ligand in **1Pb(BH$_3$)**–**5Pb(BH$_3$)** are large enough to let it seem possible that they can be isolated.

The BDEs of the diborane complexes **1Pb(BH$_3$)$_2$**–**5Pb(BH$_3$)$_2$** indicate that the second BH_3 is substantially weaker bonded except in **1Pb(BH$_3$)$_2$** and **4Pb(BH$_3$)$_2$** (Table 2). The calculated geometries and the theoretically predicted BDEs suggest that **1Pb** and **4Pb** chemically behave like divalent Pb(0) compounds (plumbylones). Note that the weakly bonded second BH_3 ligand in **2Pb(BH$_3$)$_2$** binds at the central lead atom but in the π-direction while the other BH_3 bridges the terminal Pb atoms. The BH_3 ligands are far away from each other; the boron–boron distance in **2Pb(BH$_3$)$_2$** is 4.048 Å.

6 Complexes with W(CO)$_5$ and Ni(CO)$_3$

We also optimized the transition metal complexes of $W(CO)_5$ and $Ni(CO)_3$ with **1Pb–5Pb** as ligands. The optimized geometries of **1PbW(CO)$_5$**–**5PbW(CO)$_5$** and **1PbNi(CO)$_3$**–**5PbNi(CO)$_3$** are shown in Fig. 5. The theoretically predicted BDEs are given in Table 2.

The structural features of the ligands **2Pb** and **4Pb** change little after complexation in the transition metal complexes. The cyclic NHPb moieties of **1Pb** are rotated toward a butterfly structure in the adducts **1PbW(CO)$_5$** and

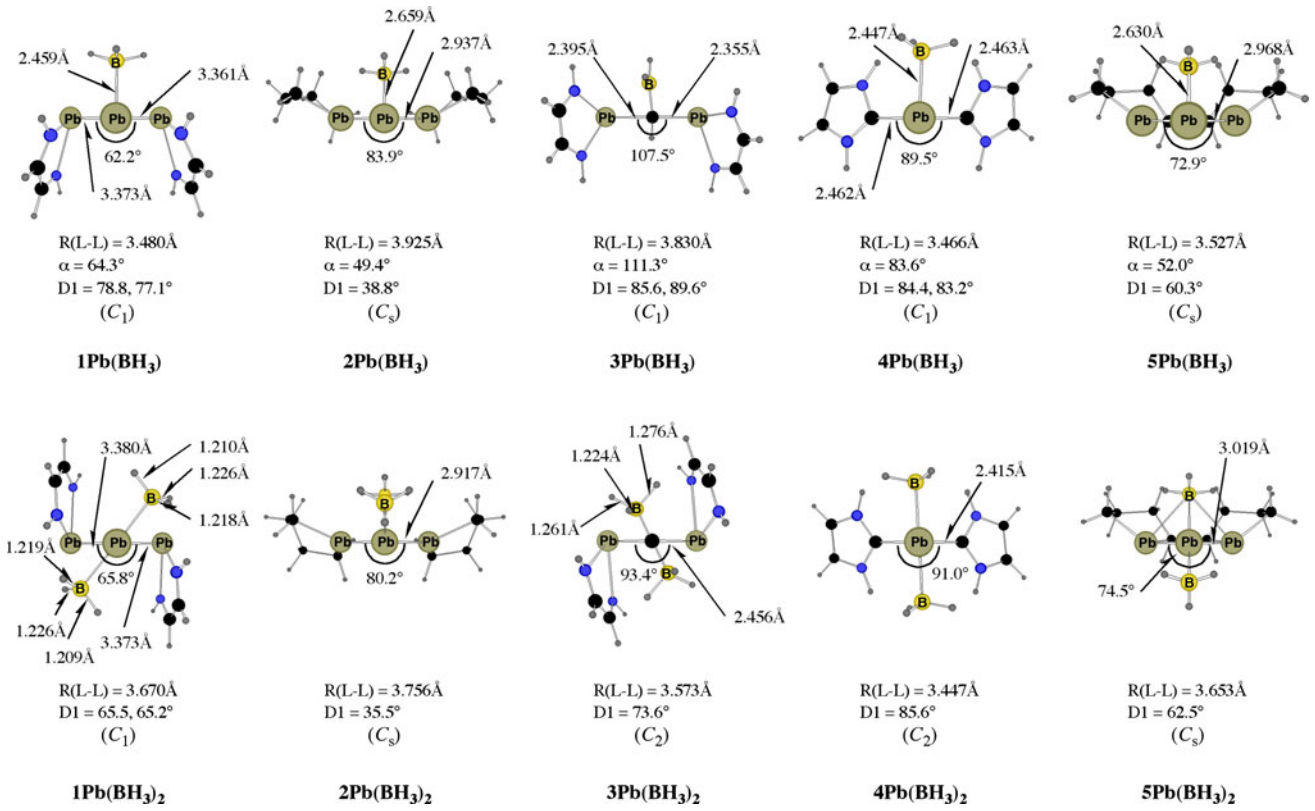

Fig. 4 Optimized geometries of the complexes with one and two BH_3 ligands **1Pb(BH$_3$)–5Pb(BH$_3$)** (top) and **1Pb(BH$_3$)$_2$–5Pb(BH$_3$)$_2$** (bottom) at BP86/TZVPP showing the most important geometrical parameters. Distances are given in Å, angles in degree. The value for R(L–L) gives the interatomic distance between the terminal lead atoms. The angle α gives the bending angle of the Pb–B bond with respect to the central E–E–E plane. For the definition of the torsion angle D1 see Fig. 1

1PbNi(CO)$_3$, but the other geometrical features of **1Pb** in the complexes are similar to those in the free ligand. The Pb–Pb bond lengths of **2Pb** and the Pb–C distances of **4Pb** become a little longer in the tungsten and nickel complexes. Note that the cyclic NHPb moieties of **3Pb** in the tungsten complex **3PbW(CO)$_5$** exhibit a similar butterfly structure as in the **1Pb** ligand in **1PbW(CO)$_5$**, while the structure of the ligand **3Pb** in the nickel complex **3NiW(CO)$_3$** changes little, except that the Pb–C distances become significantly longer (Fig. 5). The equilibrium geometries of **5PbW(CO)$_5$** and **5PbNi(CO)$_3$** are very different from each other. The tungsten complex has a T-shaped coordination of the central lead atom which has one shorter (2.909 Å) and one longer (3.185 Å) Pb–Pb bonds. The nickel complex **5PbNi(CO)$_3$** has the transition metal fragment coordinated in a π-direction to the lead atom which is also the case with all other complexes that possess a central Pb atom. The Pb–Pb bonds in **5PbNi(CO)$_3$** are slightly longer than in the free ligand **5Pb**.

Table 2 shows that the metal–ligand BDEs of the tungsten and nickel complexes are rather high. There is a regular increase in the W–E and Ni–E BDE of the systems **1E**, **3E** and **4E** with the order Si < Ge < Sn < Pb. The only exceptions are the BDEs of **1PbW(CO)$_5$** and **1PbNi(CO)$_3$** which are slightly smaller than the values for the respective tin compounds. This may be due to the large reorganization energy of the NHPb moieties in the ligands **1Pb**. The trend is remarkable because the bond strength for a bond A–B usually decreases when atom B which belongs to the same group of the periodic system becomes heavier. The opposite trend for the BDE of the metal–ligand BDEs of the tungsten and nickel complexes Si > Ge > Sn is calculated for the systems **2E** and **5E** (Table 2), but the lead species **2Pb** and **5Pb** are again exceptions. The BDEs of **2PbW(CO)$_5$**, **2PbNi(CO)$_3$**, **5PbW(CO)$_5$** and **5PbNi(CO)$_3$** are nearly as high as for the silicon compounds. The theoretically predicted BDEs D_o^{298}[W(CO)$_5$] and D_o^{298}[Ni(CO)$_3$] suggest that all complexes **1PbW(CO)$_5$–5PbW(CO)$_5$** and **1PbNi(CO)$_3$–5PbNi(CO)$_3$** should be stable enough to become isolated in a condensed phase.

7 Summary and outlook

The calculated results which are presented here suggest that the molecules **1Pb**, **2Pb** and **4Pb** possess properties

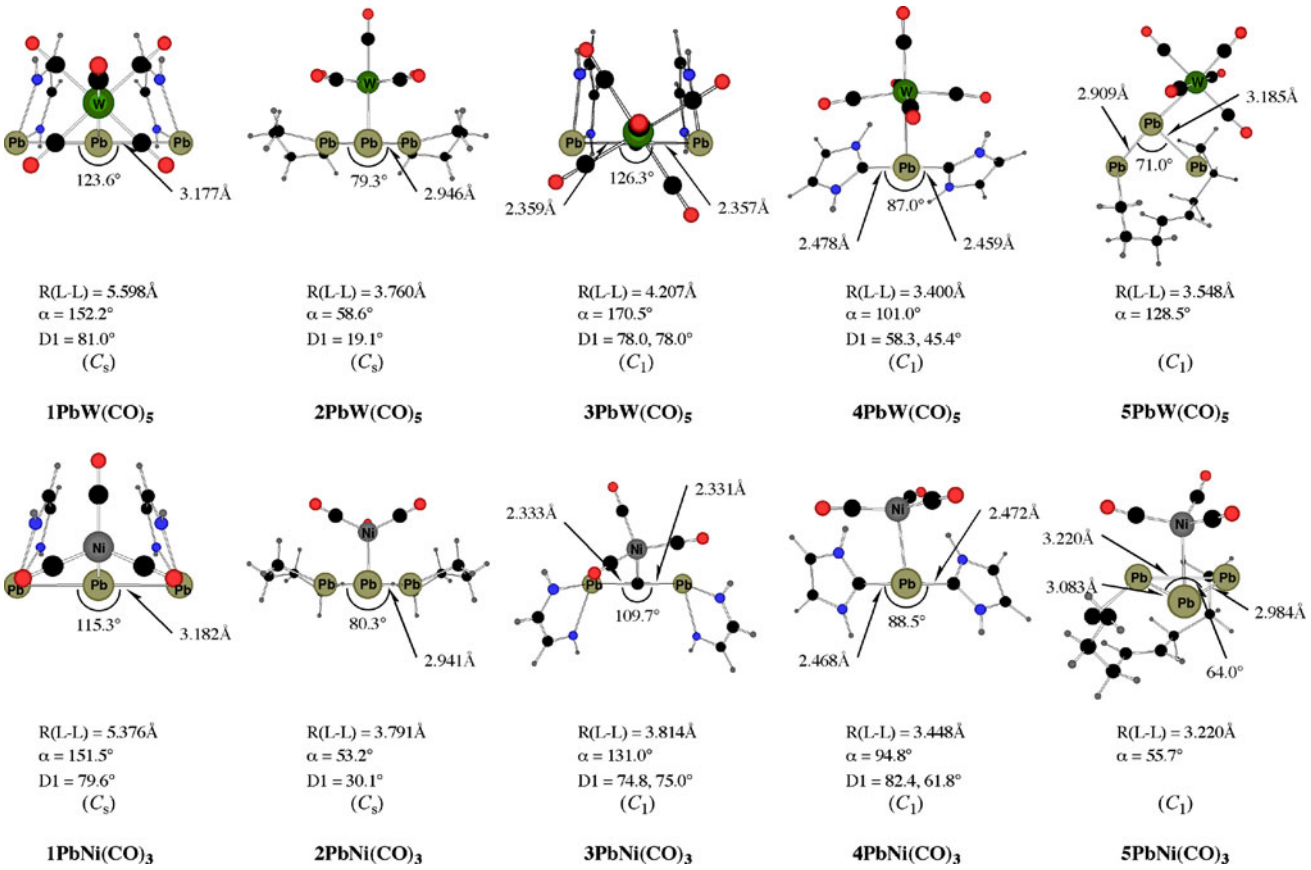

Fig. 5 Optimized geometries of the $W(CO)_5$ and $Ni(CO)_3$ complexes **1PbW(CO)$_5$–5PbW(CO)$_5$** (top) and **1PbNi(CO)$_3$–5PbNi(CO)$_3$** (bottom) at BP86/TZVPP showing the most important geometrical parameters. Distances are given in Å, angles in degree. The value for R(L–L) gives the interatomic distance between the terminal lead atoms. The angle α gives the bending angle of the Pb–W and Pb–Ni bond with respect to the central E–E–E plane. For the definition of the torsion angle D1 see Fig. 1

which identify them as divalent Pb(0) compounds (plumbylones). This comes to the fore by the theoretically predicted second PAs which are very large for a lead compound and (for **1Pb** and **4Pb**) by the BDE of the second BH_3 ligand. Compound **3Pb** should be considered as a plumbylene-coordinated divalent C(0) compound (carbone) which has a very high second PA of 195.1 kcal/mol. The geometry optimization of **5Pb** gives an equilibrium structure which identifies the molecule as divalent Pb(II) compound, i.e., as a plumbylene.

Acknowledgments This work was supported by the Deutsche Forschungsgemeinschaft.

References

1. Dyker CA, Lavallo V, Donnadieu B, Bertrand G (2008) Angew Chem 120:3250
2. Dyker CA, Lavallo V, Donnadieu B, Bertrand G (2008) Angew Chem Int Ed 47:3206
3. Fürstner A, Alcarazo M, Goddard R, Lehmann CW (2008) Angew Chem 120:3254
4. Fürstner A, Alcarazo M, Goddard R, Lehmann CW (2008) Angew Chem Int Ed 47:3210
5. Dyker CA, Bertrand G (2009) Nature Chem 1:265
6. Kaufhold O, Hahn FE (2008) Angew Chem 120:4122
7. Kaufhold O, Hahn FE (2008) Angew Chem Int Ed 47:4057
8. Jablonski M, Palusiak M (2009) Phys Chem Chem Phys 11:5711
9. Alcarazo M, Lehmann CW, Anoop A, Thiel W, Fürstner A (2009) Nature Chem 1:295
10. Patel DS, Bharatam PV (2010) Curr Sci 99:425
11. Dellus D, Kato T, Bagán X, Saffon-Merceron N, Branchadell V, Baceiredo A (2010) Angew Chem 122:6950
12. Dellus D, Kato T, Bagán X, Saffon-Merceron N, Branchadell V, Baceiredo A (2010) Angew Chem Int Ed 49:6798
13. Tonner R, Öxler F, Neumüller B, Petz W, Frenking G (2006) Angew Chem 118:8206
14. Tonner R, Öxler F, Neumüller B, Petz W, Frenking G (2006) Angew Chem Int Ed 45:8038
15. Tonner R, Frenking G (2008) Chem Eur J 14:3260
16. Tonner R, Frenking G (2008) Chem Eur J 14:3273
17. Tonner R, Heydenrych G, Frenking G (2008) Chem Phys Chem 9:1474
18. Frenking G, Tonner R (2009) Pure Appl Chem 81:597
19. Petz W, Frenking G (2010) Top Organomet Chem 30:49
20. Ramirez F, Desai NB, Hansen B, McKelvie N (1961) J Am Chem Soc 83:3539
21. Tonner R, Frenking G (2007) Angew Chem 119:8850
22. Tonner R, Frenking G (2007) Angew Chem Int Ed 46:8695

23. Klein S, Tonner R, Frenking G (2010) Chem Eur J 16:10160
24. Klein S, Frenking G (2010) Angew Chem 122:7260
25. Klein S, Frenking G (2010) Angew Chem Int Ed 49:7106
26. Takagi N, Shimizu T, Frenking G (2009) Chem Eur J 15:3448
27. Takagi N, Shimizu T, Frenking G (2009) Chem Eur J 15:8593
28. Ishida S, Iwamoto T, Kabuto C, Kira M (2003) Nature 421:725
29. Iwamoto T, Masuda H, Kabuto C, Kira M (2005) Organometallics 24:197
30. Kira M, Iwamoto T, Ishida S, Masuda H, Abe T, Kabuto C (2009) J Am Chem Soc 131:17135
31. Kosa M, Karni M, Apeloig Y (2006) J Chem Theory Comput 2:956
32. Veszprémi T, Olasz A, Pintér B (2006) Silicon Chem 3:187
33. Veszprémi T, Petrov K, Nguyen CT (2006) Organometallics 25:1480
34. Petrov KT, Veszprémi T (2008) Int J Chem Model 1:1
35. Becke AD (1988) Phys Rev A 38:3098
36. Perdew JP (1986) Phys Rev B 33:8822
37. Ahlrichs R, Baer M, Haeser M, Horn H, Koelmel C (1989) Chem Phys Lett 162:165
38. Schaefer A, Horn H, Ahlrichs R (1992) J Chem Phys 97:2571
39. Metz B, Stoll H, Dolg M (2000) J Chem Phys 113:2563